JOURNAL OF MATERIALS SCIENCE 10 (1975) 223–233

Recovery in aluminium studied by an *in situ* technique in a high voltage electron microscope

BENGT MODÉER, AGNETA ODÉN
Department of Physical Metallurgy, Royal Institute of Technology, Stockholm, Sweden

Recovery in aluminium has been studied by *in situ* technique with the aid of a high voltage electron microscope. It is shown how the dislocation density continuously decreased as the recovery proceeded. The recovery process changed the distribution of dislocation link lengths in such a way that the number of shorter links sharply decreased while there was a slight increase of the number of longer links. The observed recovery of the dislocation structure can satisfactorily be described by the dislocation network growth theory. In the formation of subgrain boundaries, high-angle grain boundaries and twin boundaries played an important role. They were often found to act as "nucleation sites" for the subboundaries. At high temperatures subgrains rapidly grew and coalesced. The growth can satisfactorily be described by analogy with the growth of dislocation network.

1. Introduction

Recovery is considered to play an especially important role in the field of high temperature creep deformation. Thus, it is generally believed that to a great extent, the overall creep process is controlled by the kinetics of the recovery process. This is supported by the fact that changes in microstructure, stress or temperature all seem to affect the creep rate entirely through the recovery process. Attempts have been made to measure the recovery during creep deformation by various techniques, and the results confirm that recovery is a determining factor in high-temperature creep deformation.

Numerous studies have been made of recovery of cold-worked metals and alloys. Various techniques have been used to follow the recovery by macroscopic parameters such as released heat, flow stress, hardness, resistivity and density. They all suffer from being indirect techniques and there must always be an uncertainty in relating these macroscopic parameters to the microscopic recovery process. Here transmission electron microscopy studies of the microstructural changes accompanying recovery have been very helpful and many such studies have been performed [1-3].

In the present study, the recovery of aluminium deformed in tension at room temperature has been followed by *in situ* recovery experiments in a HVEM operated at 1 MV. *In situ* recovery experiments have many advantages over conventional electron microscopic techniques where the process studied is interrupted at certain points and the frozen-in structure is analysed. By conventional microscopy one cannot be quite sure that the true structure is preserved and no rearrangements have taken place. By *in situ* experiments, the dynamic process can be followed as it appears and can be continuously analysed.

2. Experimental

The material used in this investigation was pure polycrystalline aluminium (99.99%) which after an annealing treatment was deformed in tension at room temperature to 5% true strain. Slices were cut out of the specimens with the aid of a spark-cutting machine, and thin foils were prepared by a conventional jet-method. The microscope used was a JEM 1000D operated at 1 MV and fitted with a heating stage which allowed heating up to 800°C. The recovery treatment was performed at 450°C ($\sim 0.75\ T_M$), a temperature which was attained within 5 min. An image recording system with a video tape recorder was used to follow and record the recovery process.

The use of high acceleration voltages enables

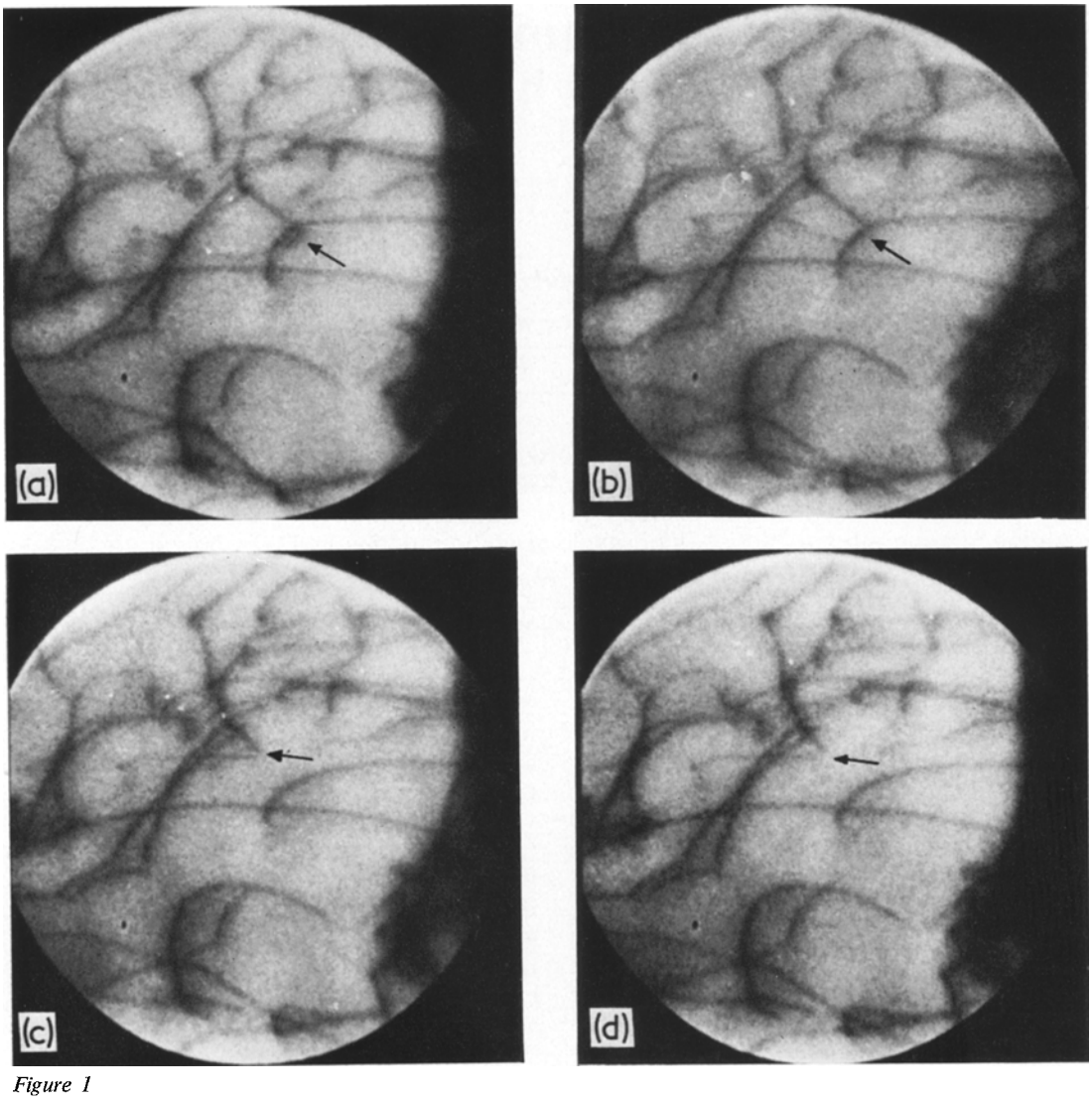

Figure 1

penetration of considerably thicker foils than in conventional electron microscopy. It has been shown [2, 4, 5] that an acceleration voltage of 500 kV enables the penetration of foils of aluminium thick enough to show the same recovery and recrystallization behaviour as bulk material. In the present case the acceleration voltage used was 1 MV and, consequently, it can be concluded that the observations made are typical of the bulk structure.

3. Results and discussion

The initial structure produced by the tensile deformation at room temperature can be characterized as a rather homogeneous dislocation structure with some tendency for tangling and cell formation. As the recovery proceeds dislocations annihilate, shorten and rearrange into subgrain boundaries, all of which will be analysed in more detail.

In the present study, the primary importance has been attached to a rather detailed analysis of rearrangements in the dislocation structure rather than to attempt to get an overall picture of the recovery process in the specimen. Thus in the following, typical behaviour of single dislocations, arrays consisting of rather few dislocations and single subgrains will be described.

Two sequences (Sections 3.1 and 3.2), will be analysed involving rearrangements in a three-

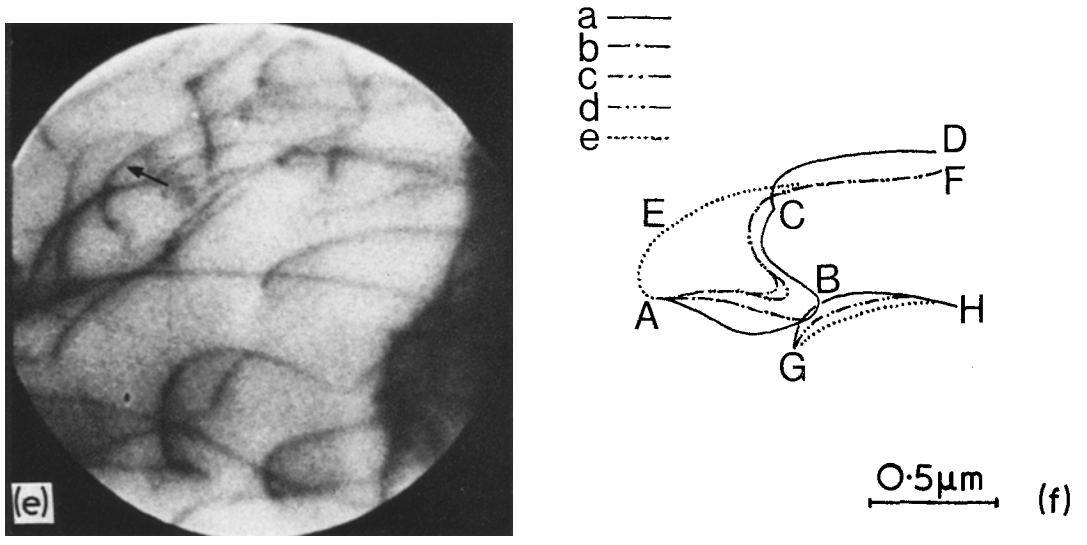

Figure 1 Sequence showing the recovery of a separate dislocation segment (ABCD). (a) $t = 0$; (b) $t = 23$ sec; (c) $t = 25$ sec; (d) $t = 26$ sec; (e) $t = 48$ sec.

dimensional dislocation structure with no cell walls or subgrain boundaries present. As the recovery proceeds, subgrain boundaries start to form and an example of this will be given (Section 3.4). At the recovery temperature used (450°C) it was not possible to detect any movement of the subgrain boundaries within reasonable time. However, when the temperature was raised to 550°C there was a pronounced rearrangement of the boundaries. At this temperature the subgrains grew rapidly, coalesced and formed new, larger subgrains, an example of which will be shown (Section 3.5).

3.1. Typical behaviour of a single dislocation

The most prominent rearrangement in the dislocation structure reproduced in Fig. 1 takes place in the centre of the pictures where the dislocation marked ABCD (see Fig. 1f) in Fig. 1a decreases its length with time and ends up in configuration AEF in Fig. 1e.

In Fig. 1a ($t = 0$) the dislocation is pinned at A either by the surface of the foil or by another dislocation not clearly observable. At B the dislocation seems to bend out around another dislocation marked GH and at C it is pinned by another dislocation. Finally the dislocation leaves the field of view at D. Fig. 1b ($t = 23$ sec), shows that segment ABC which bows out around GH has now narrowed and looks like a wide hairpin. At the same time it has approached GH at apex B, but it does not seem to have passed it. By changing its configuration it is likely that ABC increases its force on GH perpendicular to it and thereby ABC prepares to break through GH, which opposes the further shortening of ABC.

From Fig. 1c ($t = 25$ sec) we can see that the segment has now broken through dislocation GH and has passed some distance from it. Probably at the same time and as a result of this breaking, the segment CD has broken its pinning at C and has moved a short distance. The point where the dislocation leaves the field of

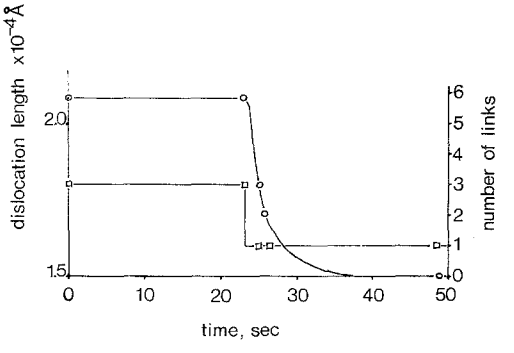

Figure 2 Dislocation length (projected) (○) and number of links (□) of the dislocation segment shown in Fig. 1, as a function of time.

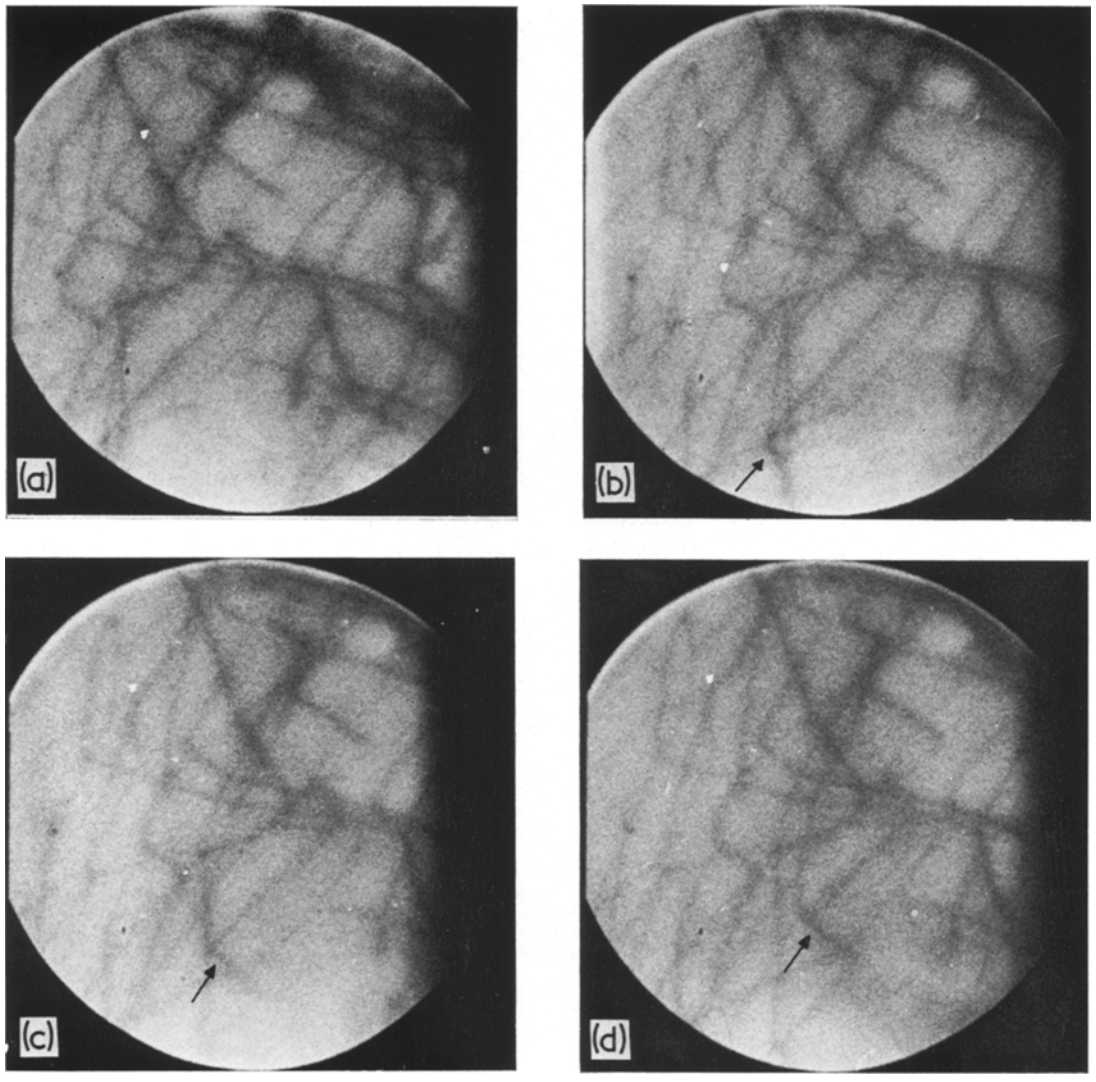

Figure 3

vision has moved down a little from D to F. The dislocation GH around which ABC originally bowed out, after the breakout is now free and starts to decrease in length.

At $t = 26$ sec (Fig. 1d) the dislocation segment ABC has further shortened in length, at the apex B, and after 48 sec, the dislocation has swung out from ABF to the new position AEF (Fig. 1e). At the same time, dislocation GH has further decreased in length.

Therefore, through the recovery process, the dislocation configuration studied has transformed from a segment composed of three links to one composed of only one, and the total length of the dislocation segment has decreased by about 30% (measured as projected length). As is clear from the above description, a close examination of a single dislocation subjected to recovery reveals that its behaviour can be characterized as a slow process during which the dislocation continuously shortens in length, probably by a climb process where the driving force is supplied by the dislocation line tension. Occasionally, a rapid shortening takes place as a dislocation penetrates a barrier in the form of another dislocation, as in Fig. 1b and c. Fig. 2 illustrates this, showing the total projected length and the number of links of the dislocation

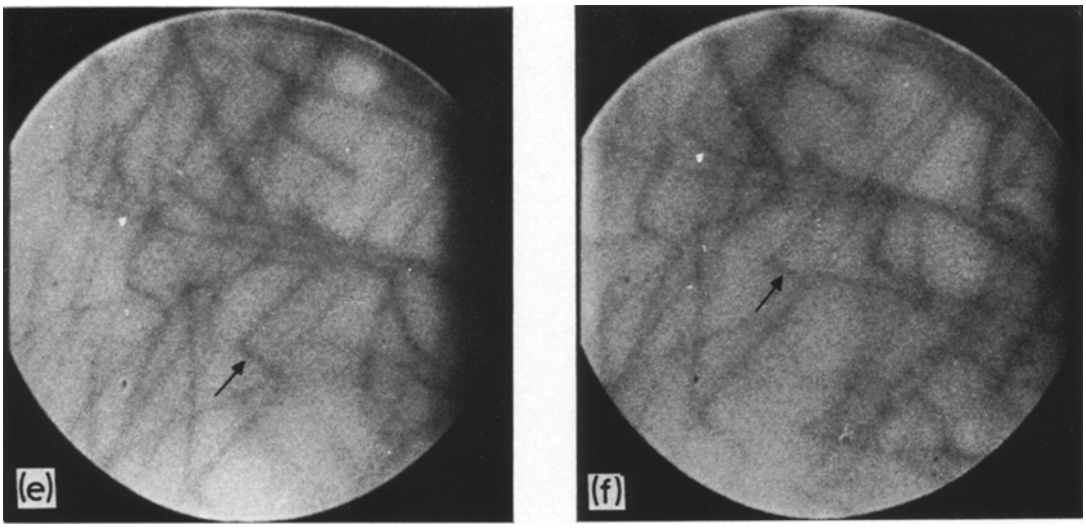

Figure 3 Sequence showing the movement of a large "jog" (arrow).

studied versus time.

Occasionally large "jogs" were found travelling through the specimen. The sequence in Fig. 3 shows an example of this (clarified by Fig. 4). The structure consists of a rather dense three-dimensional dislocation network where the dislocation links are straight as is typical of a recovered structure. In the dislocation under consideration (Fig. 4) the segment AD is straight in Fig. 3a. In Fig. 3b, however, a large "jog" BC has appeared and this continues to move upwards along AD through Fig. 3c to f as is indicated in Fig. 4. In Fig. 3e, BC has approached an obstacle in the form of another dislocation, GH, and these two dislocation segments start to interact. The motion of BC is slowed down and GH is pushed upwards a little. This is continued in Fig. 3f where BC has almost been brought to stop by the opposing GH. Fig. 5 shows the position of BC as a function of time. This illustrates clearly how the motion of BC, is unrestricted at first, taking place at a high, constant rate and is then continuously slowed down and almost stopped.

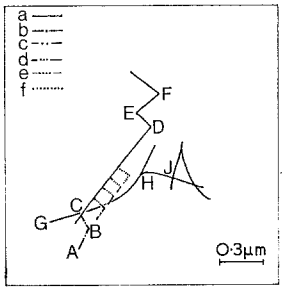

Figure 4 Schematic drawing illustrating the movement of the large "jog" BC shown in Fig. 3.

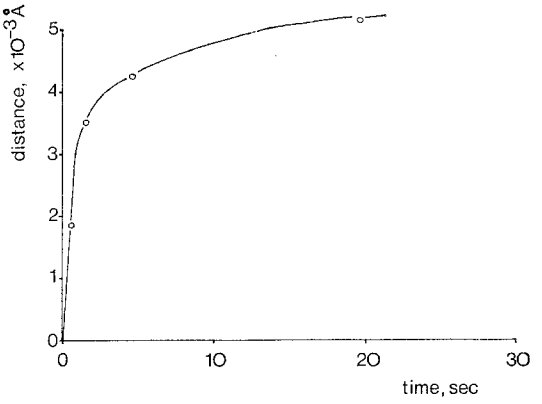

Figure 5 The distance travelled by the "jog" BC in Fig. 3 as a function of time.

3.2. Typical behaviour of a dislocation network

The series of micrographs Fig. 6a to d, shows a sequence where a loosely knit dislocation network, through the recovery, decreases its total length and the total number of dislocation links of which it is composed. Fig. 6e tries to clarify the separate events of the sequence shown in Fig. 6a to d.

Fig. 6a ($t = 0$) shows the "initial" structure. In Fig. 6e this is drawn by solid lines. The structure consists of a dislocation network with large meshes and rather straight dislocation links

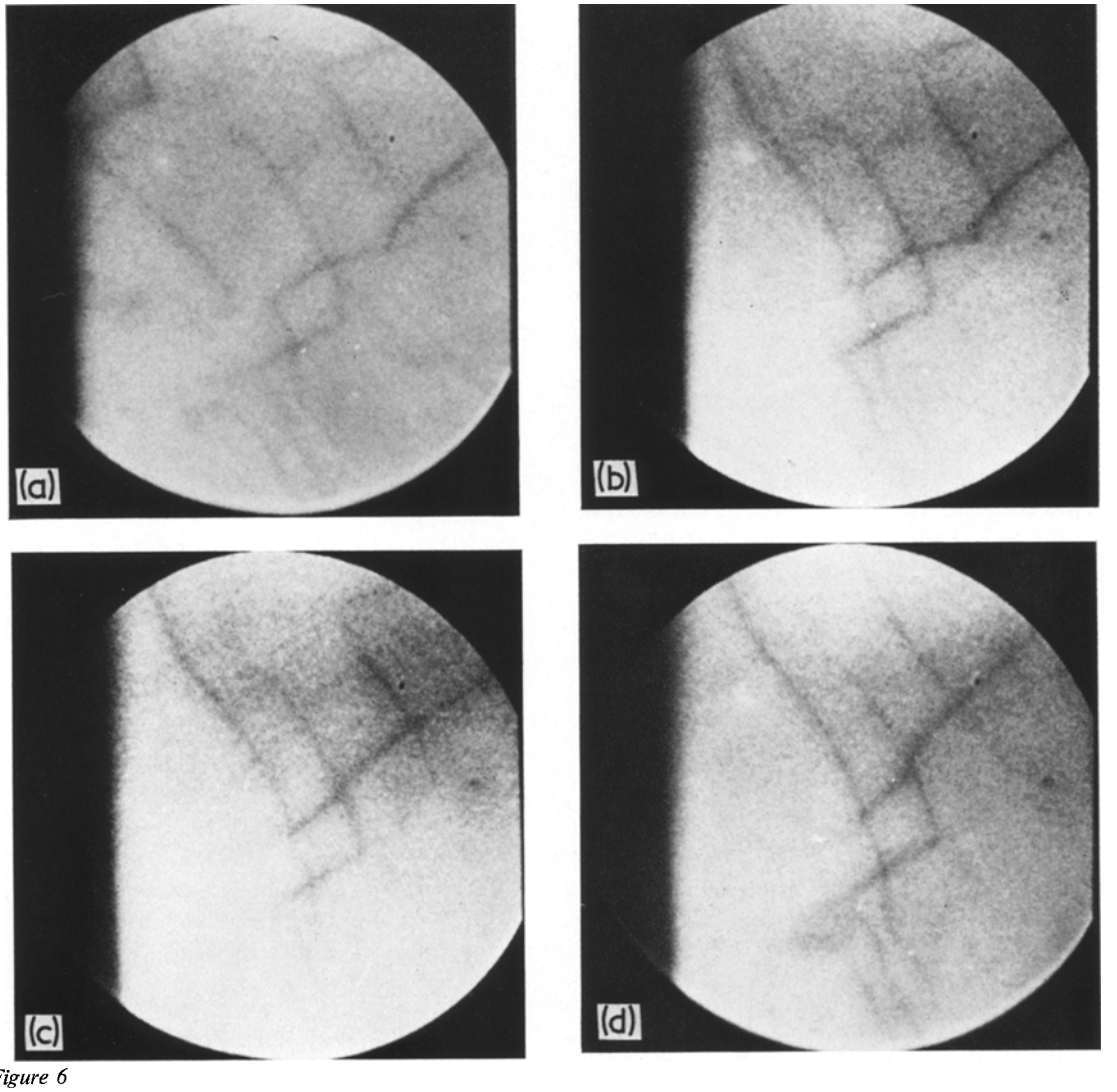

Figure 6

typical of a recovered structure. At $t = 2$ sec, the network has decreased in length by the moving of link AB to position A′B′, as seen in Fig. 6b. Fig. 6c ($t = 3$ sec) illustrates a minor rearrangement which has taken place: the segment CDE has straightened as the cusp D has been eliminated. Further rearrangement has taken place at $t = 4$ sec (Fig. 6d) the new configuration being represented by the dotted lines in Fig. 6e.

The course of events can be illustrated by Figs. 7 and 8. Fig. 7 shows the variation of the total dislocation density with time. The density rapidly drops off with time. Fig. 8 shows that as the recovery proceeds there is a pronounced decrease in the number of short dislocation links in accordance with the network growth theory [6]. A slight increase in the number of longer links is also notable. A detailed analysis by conventional electron microscopy of the distribution of dislocation links during recovery in a 20 Cr–35 Ni steel has shown the same behaviour [7]. The number of shorter links rapidly decayed while there was an increase of the number of longer links as the recovery proceeded.

3.3. Comparison with the network growth theory

Friedel [6] has proposed a model for recovery by the growth of the average mesh size in a

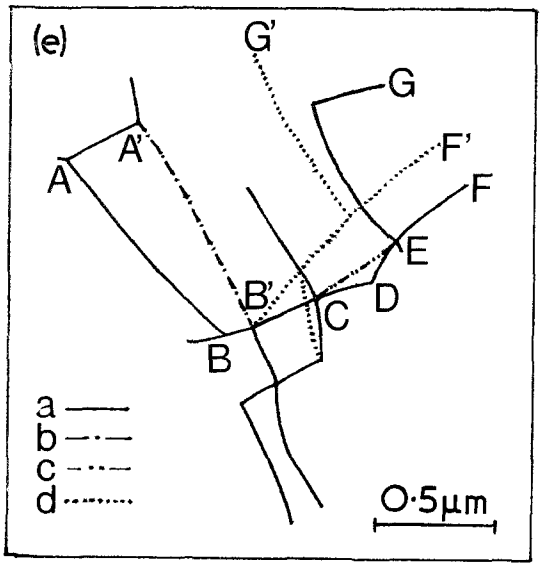

Figure 6 Sequence showing the recovery of a loosely knit dislocation network. (a) $t = 0$; (b) $t = 2$ sec; (c) $t = 3$ sec; (d) $t = 4$ sec.

three-dimensional dislocation network. The growth is assumed to occur by a climb process where the larger meshes of the network grow at the expense of the smaller in analogy with the process of grain growth. The driving force for the process is assumed to be supplied by the dislocation line tension. Thus the growth of the average mesh size R_m is given by

$$\frac{dR_m}{dt} = M\frac{\tau}{R_m}, \qquad (1)$$

where M is the mobility of the climbing dislocation and τ is the dislocation line tension.

By substituting R_m with the dislocation density according to $R_m \approx \rho^{-\frac{1}{2}}$, the following relationship is obtained:

$$\frac{d\rho}{dt} = -2M\tau\rho(t)^2 . \qquad (2)$$

The line tension τ is given by $\tau = \frac{1}{2}Gb^2$ where G is the shear modulus and $\boldsymbol{b}$ the Burgers vector. For Al, $\boldsymbol{b} = 2.8 \times 10^{-8}$ cm and G at the test temperature, 450°C, is 1.65×10^{11} dyn cm^{-2}. This gives a line tension $\tau = 6.50 \times 10^{-5}$ dyn. The mobility of a climbing edge dislocation is approximately given by [8].

$$M = \frac{D_S\boldsymbol{b}}{kT} \qquad (3)$$

where D_S is the self-diffusion coefficient. For pure Al, D_S is given by $D_S = 2.5 \exp - 34\,300/RT$ cm^2 sec^{-1} and this gives a mobility $M = 2.56 \times 10^{-5}$ cm^2 dyne^{-1} sec^{-1} at 450°C.

In the sequence in Fig. 6, a dislocation network, consisting of a limited number of dislocation links, was studied and in this case an average dislocation mesh size can be calculated and the recovery process can be analysed by the aid of Equation 1. In the time during which the

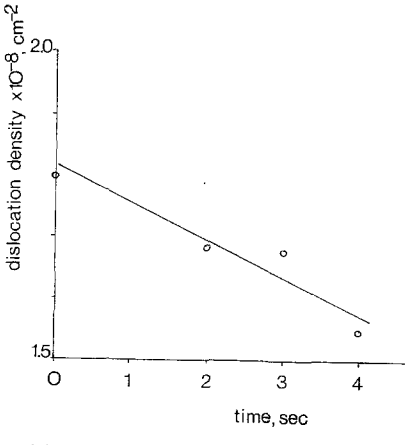

Figure 7 Dislocation density versus time for the configuration shown in Fig. 6.

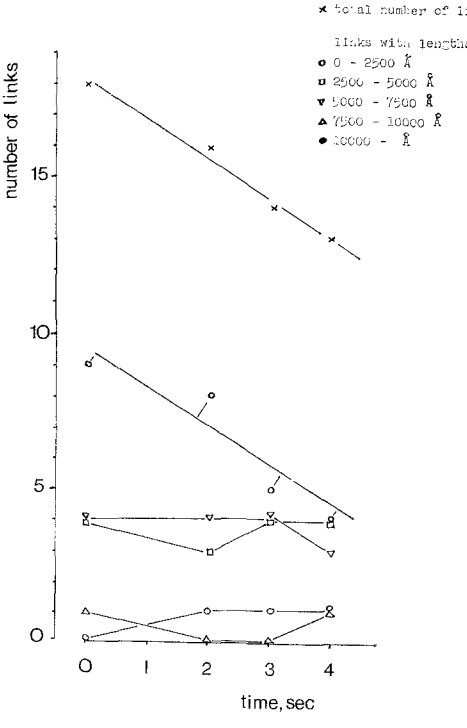

Figure 8 The change of the distribution of dislocation link lengths with time for the configuration shown in Fig. 6.

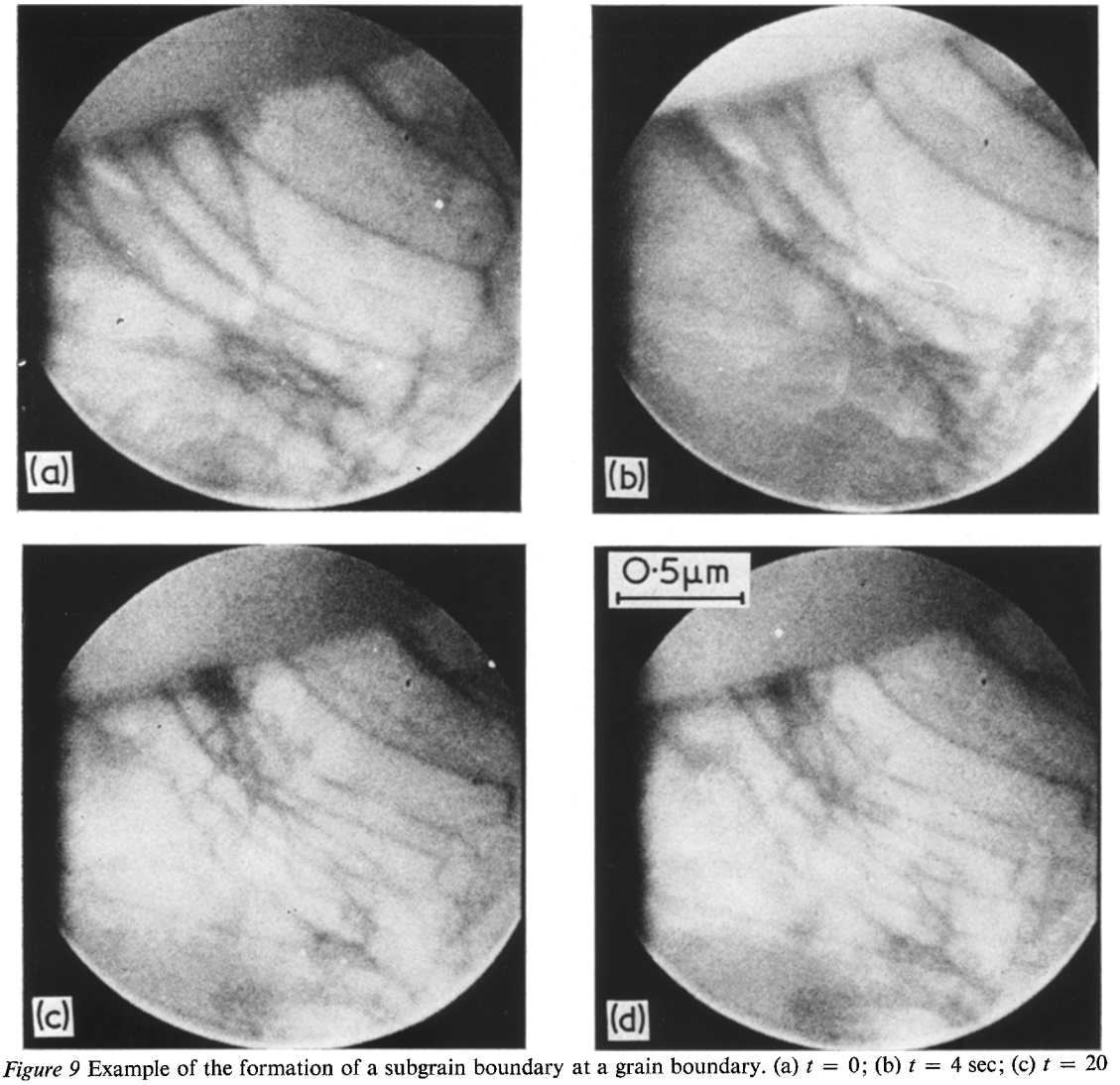

Figure 9 Example of the formation of a subgrain boundary at a grain boundary. (a) $t = 0$; (b) $t = 4$ sec; (c) $t = 20$ sec; (d) $t = 24$ sec.

network was studied, the average mesh size, R_m, increases from 3580 to 4500 Å, i.e. $dR_m/dt = 2.3 \times 10^{-6}$ cm sec^{-1}, while the theory predicts $dR_m/dt = 3.38 \times 10^{-5}$ cm sec^{-1}, a value about 15 times larger than the experimental.

For a separate dislocation link the growth rate is given by [7]

$$\frac{dR}{dt} = M\tau\left(\frac{1}{R_{crit}} - \frac{1}{R}\right) \qquad (4)$$

where R_{crit} is the critical value of R above which the link grows and below which it shrinks. In the sequence in Fig. 1, the behaviour of a single dislocation was followed. In this case an accurate comparison with Equation 4 cannot be made since the value of R_{crit} is not known. The analysis given in Fig. 8 of the dislocation structure in Fig. 6 indicates that in this case R_{crit} is about 2500 Å since the number of links with lengths shorter than this value rapidly diminishes. By using this value of R_{crit} for the analysis of Fig. 1 (which is not strictly correct since the two sequences are not taken at the same time and thus have different values of R_m and thereby also of R_{crit}), a rough comparison with Equation 4 can be made. Thus Equation 4 yields $dR/dt = 4.3 \times 10^{-5}$ cm sec^{-1}, while the experimental value is 1.5 ×

10^{-5} cm sec^{-1}, i.e. the theoretical value is about three times the experimental.

The agreement between observed and calculated mesh growth rate must be considered as satisfactory in view of the simplified expression used for M, the uncertainty in D_s and the limited study performed. However, it must be noted that in both cases analysed, the observed growth rates are smaller than theory predicts. This appears to be a general trend in all studies where the Friedel model has been applied and the climb mobility has been estimated by Equation 3. Thus in a 20Cr–35Ni steel subjected to creep deformation, calculations based on the strain-time relationship gave a mobility of about one third of that calculated from Equation 3[9]. Recovery studies on the same material [7] revealed an even greater discrepancy, the calculated value being about 30 times that observed. Direct measurements of the average dislocation velocity during *in situ* creep deformation experiments in HVEM of an Al–1% Mg alloy showed a discrepancy of the same order as does this study, the calculated value was about 4.5 times that observed [10].

3.4. Formation of a subgrain boundary

Grain boundaries were found to play an important role in the formation of subgrain boundaries. Thus subgrain boundaries frequently were found to be "nucleated" at grain boundaries, as the sequence Fig. 9a to d shows. Dislocations could often be found moving along a grain boundary with one end of the dislocation in the grain boundary as if it were hanging from a curtain hook. Fig. 9a to d shows an example of this. In the upper part of the photos there is a high-angle grain boundary to which dislocations are attached. In Fig. 9a the dislocations do not seem to show any tendency to form a subgrain boundary. In Fig. 9b, however, they have started to gather and this is continued in Fig. 9c and d. In the latter pictures the dislocations also have started to interact; they are no longer straight as in Fig. 9a.

Probably the "nucleation" of the subgrain boundary has taken place where the high-angle grain boundary possesses some kind of disturbance, i.e. a ledge or a small precipitate. It has been observed [11] that subgrain boundaries preferentially seem to occur at twin ledges.

From the dynamic observations described above, it is then quite clear how this occurs. Dislocations travel along the twin boundaries until they are caught at a twin ledge where a subgrain boundary is then formed. Earlier investigations of substructure formation during high-temperature creep deformation in rather coarse-grained materials also indicate that the initial subgrain formation may start near grain boundaries [12, 13].

3.5. Subgrain growth and coalescence

The sequence in Fig. 10a to e shows how a subgrain grows and coalesces with an adjacent subgrain to form a larger subgrain. Fig. 10f attempts to clarify the process, shown in Fig. 10a to e. In the micrographs the particle marked P provides a good point of reference.The "initial" structure is given in Fig. 10a ($t = 0$). A well-formed subgrain, called ABCDEF in Fig. 10f, lies in the centre of the picture (which unfortunately includes a disturbance from the image recording system). Most parts of the subgrain boundary seem to be of simple tilt type (i.e. part DEFA). At $t = 1$ sec (Fig. 10b) a dislocation (arrowed) has left the subgrain boundary and swung out into the otherwise empty subgrain. The part EFA of the subgrain boundary has moved outwards a little at F. At the same time this part of the subgrain boundary seems to have decreased in width. The movement of the dislocation is probably caused by an attraction from other parts of the subgrain boundary. If the dislocation density in part ABC is higher than EFA the latter will try to decompose. The dislocations constituting EFA will be exposed to an attraction from ABC and as a result dislocations may break loose, as in Fig. 10b. Fig. 10c ($t = 5$ sec) shows that the subgrain has now grown a little further, mostly at sections BC and FA, while in Fig. 10d ($t = 12$ sec), the subgrain boundary has broken at A and the two parts have moved apart a distance AA′. Thus the initial subgrain is now connected with a neighbouring subgrain and the two have now formed a larger subgrain. At the same time the widths of the subgrain boundaries have decreased noticeably. After 17 sec (Fig. 10e) a further increase in distance AA′ has taken place and the distance CD also seems to have increased a little.

The growth of the subgrain studied can be illustrated by Fig. 11 which shows the area of the subgrain versus time. For Figs. 10d and e the area within A′BCDEFA″ is plotted. If an average velocity of the movement of the subgrain boundaries is evaluated, the result is about 150 Å sec^{-1}.

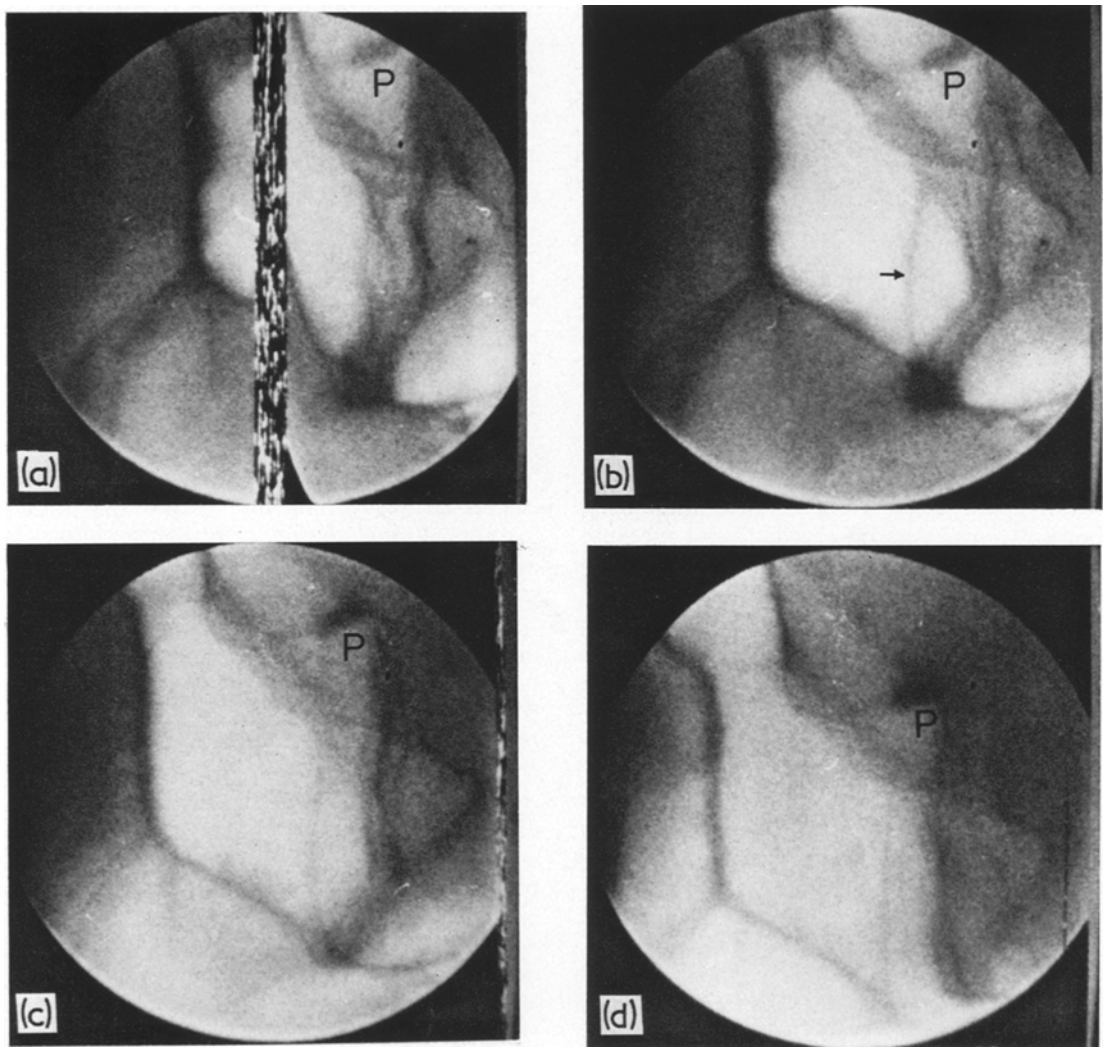

Figure 10

If the growth of the subgrain is assumed to take place by a co-operative climb of the dislocations forming the subgrain boundary and the driving force for this process is provided by the line tension of the dislocations, as in the dislocation network growth model, a theoretical estimation of the speed of the subboundary motion can be made. Assuing the subboundaries in Fig. 10 to be of tilt type and estimating the distance between the dislocations in the boundary at 5×10^{-6} cm, the line tension of the dislocations can be calculated to be about $\frac{1}{4}$ of that of a free dislocation. The mobility of the dislocations is given by Equation 3 and with a subgrain radius of 1 μm Equation 1 yields (the size of the subgrain is about the average at this time and Equation 1 should apply) $dR_m/dt = 307$ Å sec^{-1}, a value of the same order as that observed, 150 Å sec^{-1}. Thus it can be concluded that the agreement between the simple model for sub-grain growth and the observations is satisfactory.

Acknowledgements

This work was supported financially by the Swedish Board for Technical Development. B. Modéer also expresses his gratitude to the Sweden-America Foundation, Jernkontoret and the Royal Institute of Technology, Stockholm, Sweden for financial support during a stay at

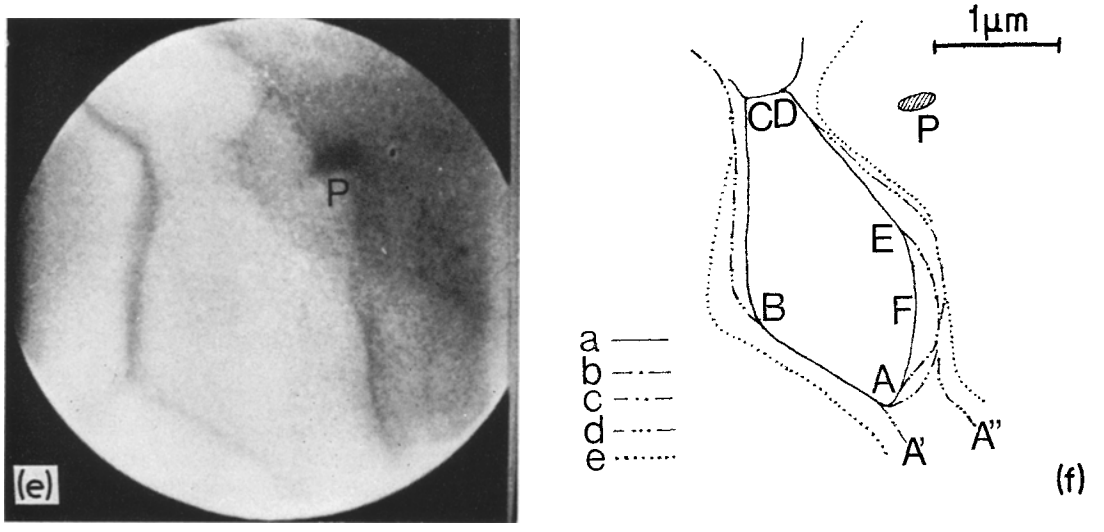

Figure 10 The growth and coalescence of a subgrain. (a) $t = 0$; (b) $t = 1$ sec; (c) $t = 5$ sec; (d) $t = 12$ sec; (e) $t = 17$ sec.

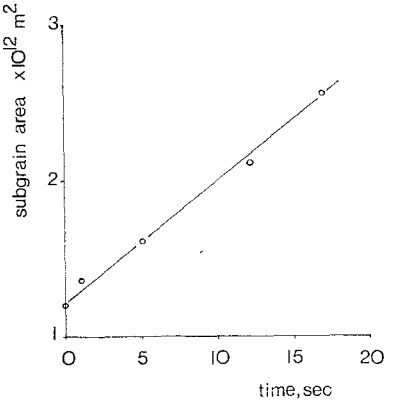

Figure 11 The area of the subgrain depicted in Fig. 10a to e as a function of time. For Fig. 10d and e the area within A′BCDEFA″ is given.

Stanford University, California, USA where a portion of this study was performed.

References

1. J. L. LYTTON, K. H. WESTMACOTT and L. C. POTTER, *Trans. Met. Soc. AIME* **233** (1965) 1757.
2. H. FUJITA, *J. Phys. Soc. Japan* **26** (1969) 1437.
3. T. V. NORDSTROM and C. R. BARRETT, *J. Mater. Sci.* **7** (1972) 1037.
4. H. FUJITA, *J. Phys. Soc. Japan* **23** (1967) 1349.
5. H. FUJITA, Y. KAWASAKI, E. FURUBAYASHI, S. KAJIWARA and T. TAOKA, *Japan. J. Appl. Phys.* **6** (1966) 788.
6. J. FRIEDEL, "Dislocations" (Pergamon Press, Oxford, 1964) p. 277.
7. A. ODÉN, E. LIND and R. LAGNEBORG, to appear in the Proceedings of the Conference on "Creep Strength in Steels and High Temperature Alloys" in Sheffield, September 1972.
8. J. P. HIRTH and J. LOTHE, "Theory of Dislocations" (McGraw-Hill, New York, 1968) p. 513.
9. B. MODÉER, Tekn. Lic. diss., Royal. Inst. Technology, Stockholm, Sweden, 1972.
10. M. HENDERSON BROWN, K. F. HALE and R. LAGNEBORG, *Scripta Metallurgica* **7** (1973) 1275.
11. B. MODÉER, to be published.
12. J. L. LYTTON, C. R. BARRETT and O. SHERBY, *Trans. Met. Soc. AIME* **233** (1965) 1399.
13. C. CRUSSARD and R. TAMHANKAR, *ibid* **212** (1958) 718.

Received 18 June and accepted 17 July 1974.